

Sensitivity of flood loss estimates to building representation and flow depth attribution methods in micro-scale flood modelling

María Bermúdez¹  · Andreas Paul Zischg² 

Received: 12 December 2017 / Accepted: 11 March 2018
© Springer Science+Business Media B.V., part of Springer Nature 2018

Abstract Thanks to modelling advances and the increase in computational resources in recent years, it is now feasible to perform 2-D urban flood simulations at very high spatial resolutions and to conduct flood risk assessments at the scale of single buildings. In this study, we explore the sensitivity of flood loss estimates obtained in such micro-scale analyses to the spatial representation of the buildings in the 2D flood inundation model and to the hazard attribution methods in the flood loss model. The results show that building representation has a limited effect on the exposure values (i.e. the number of elements at risk), but can have a significant impact on the hazard values attributed to the buildings. On the other hand, the two methods for hazard attribution tested in this work result in remarkably different flood loss estimates. The sensitivity of the predicted flood losses to the attribution method is comparable to the one associated with the vulnerability curve. The findings highlight the need for incorporating these sources of uncertainty into micro-scale flood risk prediction methodologies.

Keywords Inundation modelling · Micro-scale · Building representation · Flood loss estimation

1 Introduction

Flood inundation numerical models are a well-established approach for conducting flood risk analysis. Although one-dimensional hydrodynamic models are still in widespread use for many applications, the use of two-dimensional models is required in built-up areas to reproduce the complex, multidirectional flow paths generated by urban features (Apel et al.

✉ María Bermúdez
mbermudez@udc.es

¹ Water and Environmental Engineering Group, University of A Coruña, A Coruña, Spain

² Institute of Geography, Oeschger Centre for Climate Change Research, Mobiliar Lab for Natural Risks, University of Bern, Bern 3012, Switzerland

2009). Thanks to modelling advances and the increase in computational resources in recent years, it is now feasible to perform 2-D urban flood simulations at resolutions as low as 10 cm (Ozdemir et al. 2013; de Almeida et al. 2016). Together with the increase in data availability, this has opened up the possibility of conducting flood risk analysis and assessing damages at the scale of the single building (micro-scale), without the need for spatial aggregation of elements at risk (Staffler et al. 2008; Merz et al. 2010; Zischg et al. 2013, 2018; Fuchs et al. 2015, 2017; Röthlisberger et al. 2017). In micro-scale risk analyses, flood hazard is estimated by means of spatially detailed models solving the 2D shallow water equations. In addition, fine-resolution geospatial datasets are exploited to characterize the reconstruction value and the vulnerability of each building. Such a detailed analysis is relevant to reliably assess the effectiveness of flood protection measures for reducing flood risk in individual areas (Ernst et al. 2010). It can be used to objectively evaluate the economic cost-effectiveness of individual precautionary measures on buildings (i.e. retrofitting methods) (Arrighi et al. 2013), or be part of decision support systems to evaluate flood risk (Qi and Altinakar 2011).

The adoption of a micro-scale flood modelling approach allows the representation of small-scale structural elements and small topographic variations explicitly in the hydrodynamic model, instead of parameterizing their effects via subgrid scale models or artificial roughness (Abdullah et al. 2012; Abily et al. 2016). The value of roughness coefficient in such a 2D hydrodynamic model is thus set to represent only small-scale roughness, its calibration being less important than for low spatial resolution models (Horritt and Bates 2002). This is relevant because of the lack of sufficient data for model calibration and validation in many locations. However, sensitivity to other model features, such as the mesh set-up in relation to the building pattern and the building representation, may have a significant impact on the hydrodynamic results and, in turn, on the flood loss results. A few studies deal with these effects in urban areas (Fewtrell et al. 2008, 2011; Sampson et al. 2012; Schubert and Sanders 2012). However, these aspects have received far less attention for rural and peri-urban situations and have been generally explored in isolation from evaluation of uncertainties in loss estimation approaches.

Several methods have been proposed in recent years to represent buildings in shallow water models. A first group of methods parameterizes the effects of buildings on flooding by means of porosity parameters (Cea and Vázquez-Cendón 2009; Schubert and Sanders 2012; Guinot 2012) or by building coverage and conveyance reduction factors (Chen et al. 2012a, b). This allows the simulation of urban flood flows with a relatively coarse mesh and hence a fast execution time. However, these methods are not suitable for micro-scale flood modelling, which aims at capturing the localized variability of flood depth and velocity around buildings. In this case, a so-called resolved approach, which explicitly considers the exact building geometries, is needed (Schubert and Sanders 2012). The building block (BB) method and the building hole (BH) method are among the most used methods of this type. In the BB method, a digital surface model that incorporates the heights of the rooftops is used to produce a local elevation rise of the grid cells within building footprints. In the BH method, the area within the building footprints is excluded from the model domain, and closed boundary conditions are enforced at building walls. As noted by Bellos and Tsakiris (2015), reservations have been expressed for the BB and BH methods, related to the fact that they do not simulate flood flow inside the building and therefore any possible storage effects of the buildings are not taken into account. However, alternative methods such as the representation of the exterior walls of each building with an inlet on the front wall (Bellos and Tsakiris 2015), so that water can slip into the house, are seldom used in practical applications.

A key component of any flood risk analysis is the vulnerability assessment (Fuchs et al. 2012; Papathoma-Köhle et al. 2017) which is frequently focused only on direct flood loss. Depth-damage functions, which denote the flood damage that would occur at specific water depths per asset or per land-use class, are typically applied for this purpose. Other factors such as flow velocity are presumed to influence flood damage, but their general consideration in monetary loss modelling is not recommended (Kreibich et al. 2009). From a practitioner's perspective, the application of depth-damage functions is, therefore, the standard approach to assessing urban flood loss. The development of site-specific depth-damage functions is not feasible at many locations, and the use of models developed elsewhere is common practice in the literature (Apel et al. 2006; Notaro et al. 2014). In fact, libraries of depth-damage curves are available for different regions (Davis and Skaggs 1992; Green 2003). In addition to the inherent uncertainty in the depth-damage curves, their extrapolation to regions where building characteristics are not necessarily the same raises concerns regarding their local representativeness (Cammerer et al. 2013; McGrath et al. 2015). Various studies have already acknowledged the uncertainty and limitations associated with the use of depth-damage curves in flood damage estimation (de Moel and Aerts 2011; Sampson et al. 2014). Freni et al. (2010) suggest that the use of highly detailed 2D hydraulic models in flood risk assessments might not be justified if depth-damage curves are used to assess damages, given the significant uncertainties of the later.

In addition to the selection of a suitable depth-damage curve, other modelling choices need to be made in flood risk assessments. It is necessary to define how the number of exposed buildings will be counted and how the inundation characteristics will be assigned to each exposed building. Exposure information is essentially provided through the overlapping of the building footprint and the hazard maps. The high spatial resolution of the hazard results in micro-scale flood assessments allows, however, for different exposure evaluation, i.e. building counting, methods. A building can be assumed to be affected by the inundation if water depths computed within its footprint are above a certain wet-dry threshold. More sophisticated methods consider a buffer distance between the building edges and the flooded areas or calculate the proportion of the external perimeter of a property that is wet in the case of partially flooded buildings (Environment Agency 2014). On the other hand, the assignment of flow characteristics (water depths in the general case) to each building may be performed in different ways. This is referred to as flow depth attribution method in this paper. In the micro-scale flood risk analysis performed by Ernst et al. (2010), the water depth in the building is obtained either by averaging the water depth in the neighbouring cells or by linearly interpolating the ground level and the free surface elevation inside the asset. The aforementioned differences in attribution methods can potentially result in very different flood damage estimates. Yet, to the best of our knowledge, there are no studies available that have quantified its impact on the flood loss predictions.

Hence, the main research question for this paper is how flood loss estimates are influenced by the building representation and the flow depth attribution methods. To answer this question, we conduct a micro-scale flood loss assessment in a low-density residential case study that is typical for rural and peri-urban hilly landscapes in Europe. The modelling framework comprises a flood inundation model and a flood loss model, which provide hazard and impact estimates for a given flood event at a high spatial resolution. We analyse the sensitivity of the predicted flood loss to the building representation in the flood inundation model and to the vulnerability function and attribution method in the flood loss model. The benefits and limitations of the different methods are evaluated, and the applicability for real-world case studies is discussed. The main aim of

this work is to contribute to the development of consistent frameworks for micro-scale flood risk assessments, with a balanced accuracy and spatial detail of the different steps of the modelling process.

2 Methods

The model experiment was set up on the basis of a flood inundation model and a flood loss model (Fig. 1). Both sub-modules were altered in the experiment. While we kept the upstream boundary condition of the flood inundation model constant, i.e. the inflow hydrograph, we varied the computational mesh with different representations of the buildings. In the flood loss module, the building dataset was kept constant while we varied the flow depth attribution methods and the vulnerability functions. The methodology is described in more detail below.

2.1 Study area

We set up the model experiment in the case study of Steffisburg, a community in the Canton of Bern in Switzerland. The study area covers an area of 4.8 km² and is located on the alluvial fan of the Zulg River (Fig. 2). The fan has an average slope of 1.3%. The Zulg River has a catchment area of 90 km². The main village of Steffisburg is located along the Zulg River sprawling towards south and the city of Thun. It has 15,700 inhabitants and 1682 buildings. The density of buildings is low in comparison with urban areas (~ 350 buildings per km²) but not as low as in rural areas. The average distance between three neighbouring buildings is 14.4 m with a standard deviation of 12.6 m. In comparison, Schubert and Sanders (2012) computed an average gap between buildings in an urban environment of 3.8 m. Hence, the village can be classified as a typical peri-urban settlement. The majority of the buildings are of residential and combined residential/commercial use. In the south and the north of the study area, two clusters of industrial/commercial buildings are located.

2.2 Flood inundation model

A flood inundation model of the area was set up using the software Iber (Bladé et al. 2014). The model solves the 2D depth-averaged shallow water equations by means of a finite

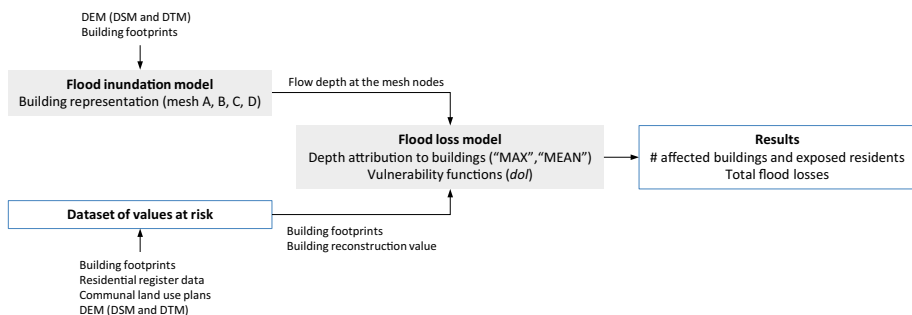


Fig. 1 Flow diagram of the methodology: flood inundation model, flood loss model and dataset of values at risk

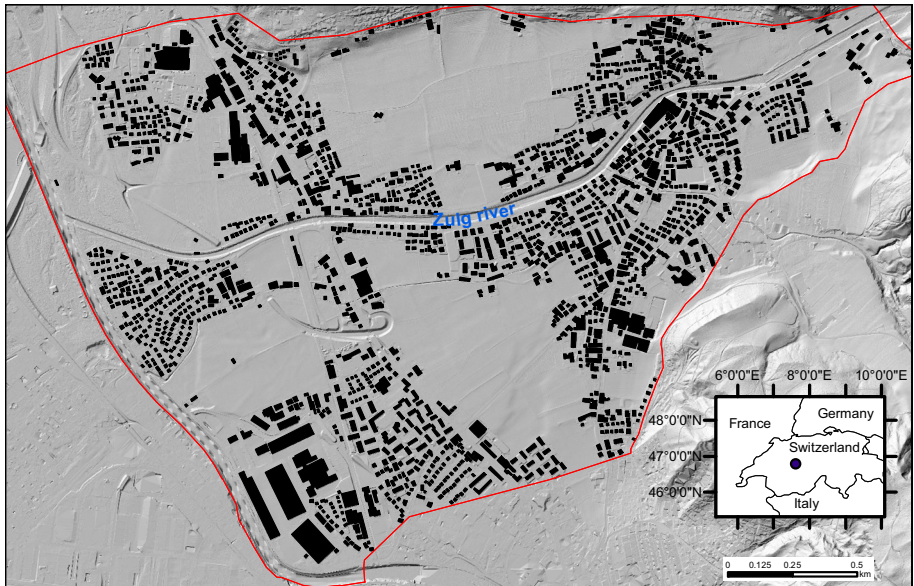


Fig. 2 Extent of the study area. The Zulig River flows from NE to W through the village of Steffisburg

volume method. It computes the water depth and the two horizontal components of the depth-averaged velocity, the former constituting the basis for the flood hazard assessment in this work. The model Iber has been successfully applied in a wide range of flood modelling studies (Bodoque et al. 2016; González-Aguirre et al. 2016; Álvarez et al. 2017; Bonasia et al. 2017), including detailed flood assessments in urban areas, in which the flow depth field was evaluated at the scale of the streets and buildings (Garrote et al. 2016; Bermúdez et al. 2017). For a detailed description of the model and additional validation examples, we refer to Bladé et al. (2014) and Cea et al. (2016), and the references therein. The model is run in an uncalibrated mode using typical physical values for the Manning roughness coefficient, as proposed by Zischg et al. (2018). This is justified due to the low sensitivity of the model to the friction parameter and the absence of documented flood events that could be used for validation.

We set up the flood inundation model at the micro-scale, which implies that exposure and hazard must be assessed at the scale of individual elements at risk such as buildings or infrastructures. The flood model must, therefore, represent flows at this targeted spatial scale. The domain was discretized accordingly by an unstructured computational mesh at a very high spatial resolution, with mesh sizes of 2.5 m in the built-up areas and the river channel, and between 5 and 10 m in the non-urbanized areas. Element size is thus smaller than the critical length scales determined by building dimensions and building separation distances (Fewtrell et al. 2008). The total number of elements in the mesh is approximately 1,000,000, the exact number is depending on the mesh set-up explained below. We used a 0.5-m resolution digital elevation model (DEM) derived from LiDAR and a building footprint map to define the model geometry. Two different DEMs were used in this study: a “bare-earth” digital terrain model (DTM) and a digital surface model (DSM) which incorporates the elevation of the buildings (i.e. the heights of the rooftops). Four different

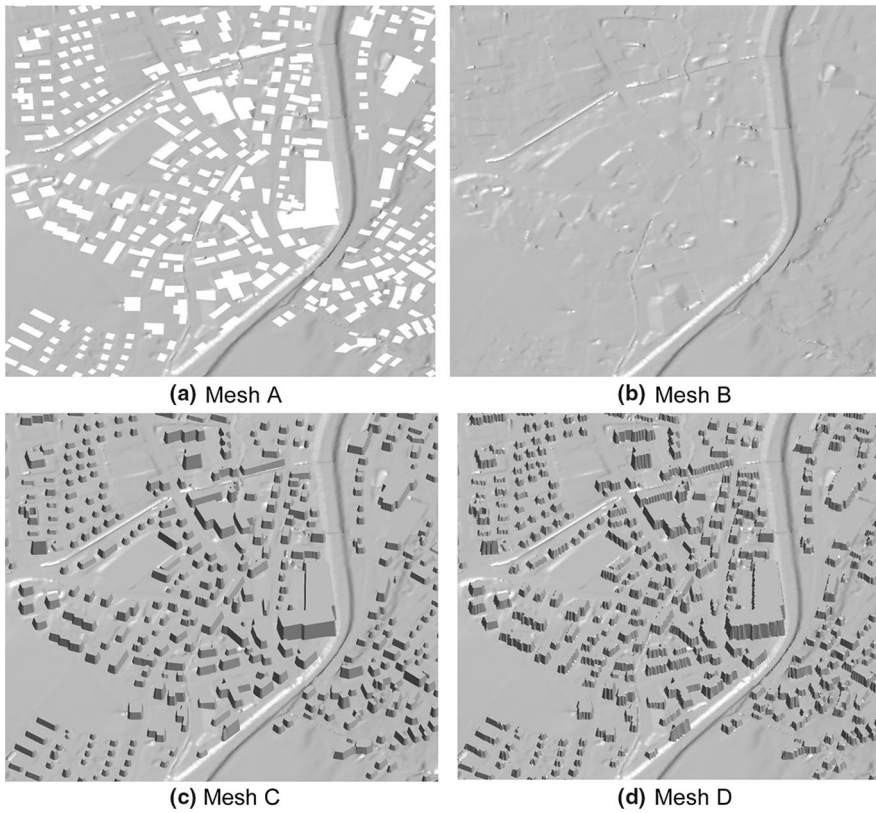


Fig. 3 Mesh geometries with different representations of the buildings (3D view). In **a**, buildings are represented as holes, while in **b–d** the area covered by the buildings is part of the mesh. The z -coordinates of the nodes within the building footprints equal the values of the DTM in **b** and the values of the DSM in **c** and **d**

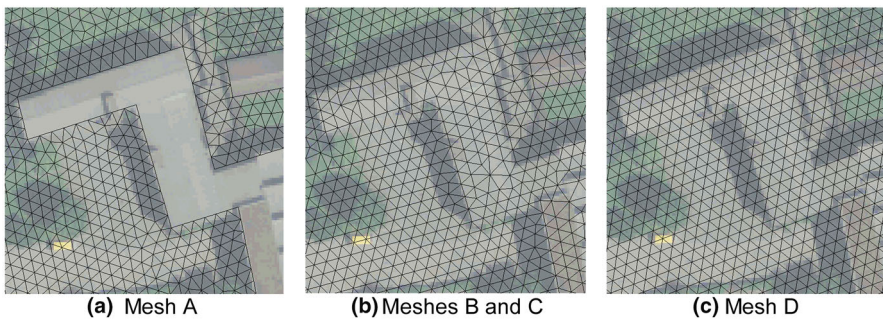


Fig. 4 Detail of the mesh around a building, overlaid on an aerial image. Meshes B and C are identical in this plan view, although elevations assigned to the nodes within the building footprint differ. Building footprints serve as constraints for mesh generation in meshes A, B and C

mesh configurations were considered (Figs. 3, 4), which differ on the building representation, as follows:

- *Mesh A* The building hole method BH is used to represent the buildings. Buildings are thus void areas in the mesh and buildings' walls fit exactly with numerical mesh edges.
- *Mesh B* Buildings are not represented in the model. For this purpose, the area covered by the buildings is not excluded from the calculation domain and the topography is defined from the DTM. The building footprint is still used to generate the mesh, so the mesh nodes located in the building walls stay at the same location as in mesh A.
- *Mesh C* The building block method BB is used to represent the buildings. This means that the buildings are not excluded from the calculation domain, and they appear as blocks with the height of the roofs in the mesh. The building footprint is used to generate the mesh, so building walls are aligned with internal element edges in the mesh (Fig. 4b). This allows a precise representation of the contours of the buildings in the mesh, as shown in Fig. 3c.
- *Mesh D* The building block method BB is used to represent the buildings, as in mesh C. However, the building footprint is not used to create the mesh, so mesh nodes are not forced to lie along the building footprint (Fig. 4c). As a consequence, the mesh cannot fit exactly the walls of the buildings, no matter how fine the resolution of the mesh is. Building walls are thus subject to an effect similar to the "staircase effect" that appears at curved and slanted interface boundaries on regular Cartesian grids (Kumar et al. 2009), as can be seen in Fig. 3d.

2.3 Values at risk

In this study, we focus on losses to buildings. Damages on house content, infrastructure or indirect losses are not considered. Hence, the dataset of the values at risk consists of a spatial dataset representing the buildings and their characteristics. The building is spatially represented by its footprint polygon. This basic dataset was extracted from the terrain model of the Federal Office for Topography (swisstopo). Adjacent polygons were merged to one polygon. We attributed the data of the residential register to the building footprints. These data were provided by the Federal Office for Statistics. This results in the number of residents per building. With this dataset, it was possible to classify all buildings with residential purpose. In a further step, we attributed the land-use categories of the communal land-use plans to each building. This leads to a distinction between buildings with residential, commercial, industrial and public purpose. Moreover, we attributed the volume of the building by computing the average difference between DSM and DTM and multiplying it with the footprint area. The reconstruction value of each building was successively computed on the basis of the volume and a typical price per volume differentiated by building category. The approach followed the methods presented in Fuchs et al. (2015, 2017) and Röthlisberger et al. (2017).

2.4 Flood loss model

The flood loss model combines the outcomes of the inundation model with the dataset of the values at risk. To allow the assessment of the uncertainties in the methods for representing the buildings in the mesh and in the methods for attributing flow depths to the buildings, the flood loss model has to be designed in a flexible way. The spatial representation of the buildings by their footprints is held constant in all methods for pre-

processing the mesh. However, depending on the representation of the buildings in the mesh, the flow depth attribution method changes. Thus, the flood loss model allows to consider different set-ups. In all set-ups, a building is counted as affected by the flood process if (a) a mesh node within the building footprint or (b) a mesh node at the border of the building footprint has a flow depth > 0 . In addition, the model allows the consideration of a building as affected if (c) a mesh node within a user-defined buffer distance is modelled as wet.

To account for the different building representation methods in one flood loss model, we set up the procedure described in the following steps. In a first step, the computational mesh of the Iber flood model is read in and a point dataset of nodes is created. Second, the nodes point dataset is intersected with the building footprint dataset and a topology table is created. Herein, two situations can be handled. The intersection between both datasets results in a new point dataset. This dataset contains all buildings that have nodes of the computational mesh located within its footprint polygon. All other buildings not having any nodes located within their footprints are considered in a further step. For these buildings, a near table is computed by considering a maximum buffer distance and a maximal number of nodes to consider in the neighbourhood analysis. This results in a table listing the mesh nodes that are relevant for attributing the flow depths to the building. The buffer distance and the maximum number of points to be considered in the analysis can be defined by the user. In our study, we defined a search radius of 0.5 m and a maximum number of 100 nodes to consider in the neighbourhood analysis. Third, the simulation outputs of the Iber model, i.e. the flow depths per mesh node and time step, are read into an array.

For each building, it is iteratively searched in the topology tables if the building intersects directly or indirectly (neighbourhood) with the mesh nodes. If the intersection between building and mesh nodes is a direct overlay, the flow depth is directly attributed to the building from the flow depths located within the building footprint. This can be done either by computing the average (MEAN) or the maximum flow depth of all nodes (MAX). If the building has no mesh nodes within its footprint, the flow depth is attributed from the neighbouring mesh nodes. Herein, also the average or the maximum could be defined depending on the research question. However, in the case of the “MEAN” attribution method, the average is computed by inversely weighting the distance between the building and the mesh nodes. The flow depth attribution is done for each time step of the flood inundation simulation. Consequently, a flow depth hydrograph is extracted for each building. In a subsequent step, the maximum flow depth over all time steps for each building is used to compute the degree of loss by means of the vulnerability function.

In this study, we used the vulnerability functions of Totschnig et al. (2011), Papathoma-Köhle et al. (2015), Hydrotec (2001), as cited in Merz and Thieken (2009), Jonkman et al. (2008) and Dutta et al. (2003). We used different vulnerability functions because, on the one hand, we aim at assessing the uncertainties in this part of the flood loss model and, on the other hand, we do not have loss data to validate the loss function or to choose the function with the highest fit. However, each of the selected vulnerability functions allows us to delineate a degree of loss for each building depending on the magnitude of the flood, i.e. the flow depth at the building scale in our case. The degree of loss *dol* resulting from the vulnerability function and the flow depth is used to compute the loss of the building. This is done by multiplying the *dol* with the reconstruction value of each building. Finally, all losses computed at single building level are summed up at the level of the study area.

With these specifications, the flood loss module is able to consider all four approaches for representing the buildings in the loss modelling. In mesh A, only the mesh nodes within

a distance of 0.5 m from the outline of the building footprint are considered in the flow depth attribution. In meshes B, C, and D, the mesh nodes within the building footprint or within a distance of 0.5 m from the outline are considered.

3 Results and discussion

The application of the flood loss model on the outcomes of four different flood inundation models, combined with two flow depth attribution methods and five vulnerability functions, resulted in forty simulation results. The number of affected buildings ranges from 572 to 618, and the number of exposed residents ranges from 3373 to 3502. The results of the exposure analyses are shown in Table 1. Mesh set-up D shows the lowest numbers of exposed buildings and residents, while mesh A shows the highest. Although the variability in the exposure is below 8%, this demonstrates that the procedure is sensitive to the mesh set-up and the approach of representing the buildings in the mesh.

Differences in flood extent between meshes A, C and D, which include different representations of the buildings, are below 0.3%. On the other hand, mesh B shows an increase in the flooded area of around 10% with respect to the other mesh configurations. However, given that buildings are not represented in mesh B, the internal area of affected buildings is counted as flooded area.

In contrast to the flood exposure, the flow depths at single building vary markedly with the mesh set-up and the flow depth attribution method. Figure 5 shows a comparison between the mesh set-ups and the flow depth attribution method. Obviously, the “MAX” flow depth attribution method results in higher flow depths at building scale than the “MEAN” method. The differences are particularly high for mesh C and mesh D, given that the dry nodes within the building footprint (nodes with the height of the rooftops) are used in the calculation of the mean depth of the building. In these cases, the “MEAN” method underestimates flow depths. In an additional calculation, we removed the nodes within the buildings and counted only the nodes at the outline of the building footprint in meshes B and C, or the neighbouring mesh nodes in mesh D. If the nodes within the building are excluded from the flood loss calculation, the flow depths are higher and more similar to the ones computed with mesh A (see Table 2). In the case of mesh B, the difference with the original mean depth value is very small, given that the nodes within the footprint are assigned the height of the ground and can thus be flooded. This leads to the conclusion that in averaging the flow depths (“MEAN” attribution method), the nodes within the building footprints should be excluded if their *z*-coordinates represent the building heights (BB method) and consequently do not exhibit relevant flow depths.

Table 1 Flood extent, number of exposed residents and number of affected buildings with the different mesh configurations

Mesh	Flood extent (m ²)	# Affected buildings	# Exposed residents
A	1,107,339	618	3502
B	1,242,711	592	3447
C	1,107,045	589	3391
D	1,110,062	572	3373

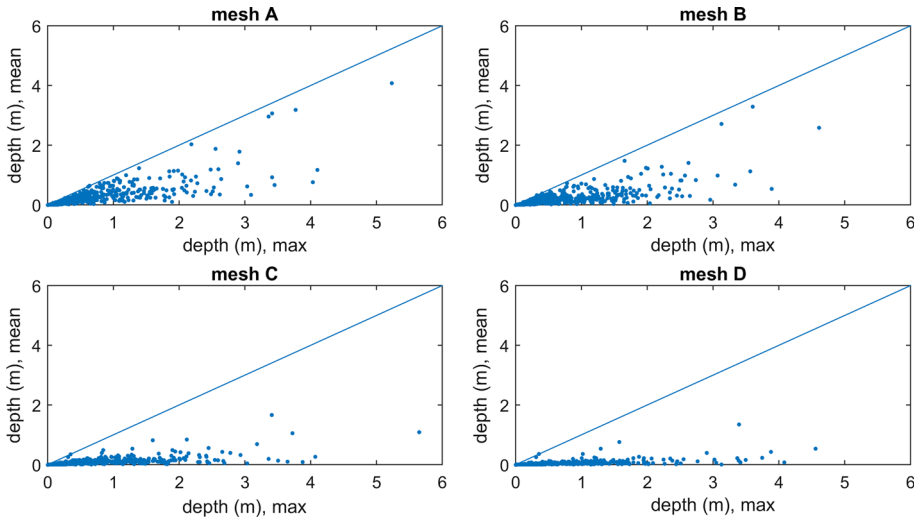


Fig. 5 Scatter plot of depth values assigned to each building with the different hazard attribution methods

Table 2 Average depth (m) attributed to buildings

Mesh	Flow depth (m) “MAX” attribution method	Flow depth (m) “MEAN” attribution method	Flow depth (m) “MEAN” attribution method (nodes within buildings excluded)
A	0.623	0.248	Not applicable
B	0.624	0.190	0.192
C	0.667	0.088	0.242
D	0.655	0.046	0.263

On average over all buildings, the flow depths attributed to the buildings by the “MAX” attribution method are systematically and markedly higher than the ones computed with the “MEAN” method. It should be noted that differences are also very relevant for mesh A, which has no nodes within the building footprints, and for mesh B, in which the nodes of the building footprint are assigned the height of the ground and can thus be flooded. In this relatively steep study area, the range of z -coordinates at the outlines of the building footprints (i.e. the difference between the minimum and maximum altitudes of the building footprint) is 0.78 m on average. Large buildings have a length of up to 80 m, which results in an altitude difference of up to 8.8 m. This significant variation in z -coordinates across the footprints results in variable flow depths within a single building. A significant portion of all buildings is only partially wet. It is concluded from the above that, as the flow depth is relevant for the computation of the degree of loss, the flood loss computation is highly sensitive to the flow depth attribution method.

When comparing the flow depths at building scale of the different mesh set-ups, the relevance of the flow depth attribution method becomes obvious again (see Fig. 6). However, the “MAX” attribution method has a relatively low sensitivity to the mesh set-up. The flow depths assigned to buildings are very similar for all four mesh set-ups. In

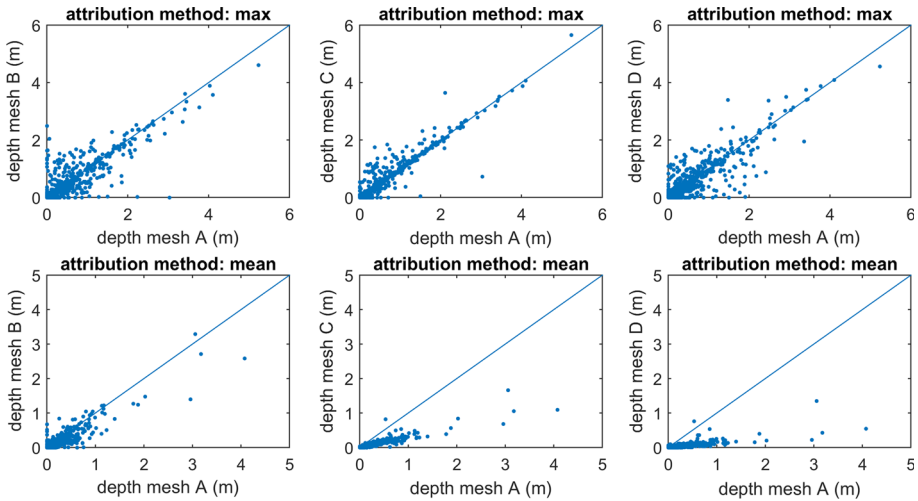


Fig. 6 Scatter plot of depth values assigned to each building with the different mesh configurations

contrast, the “MEAN” attribution method implies a higher sensitivity as meshes C and D result in significantly lower depths in buildings than meshes A and B. The averaged flow depths (“MEAN”) differ markedly between the mesh set-up, whereas the maximum flow depths (“MAX”) do not vary significantly. Hence, the latter flow depth assignment method produces robust estimations. It should be noted, however, that this robustness does not imply that the accuracy of the method is necessarily superior. If flow depths vary significantly across a single building, the depths obtained with the “MAX” attribution method might not be representative for damage assessment and produce an overestimation of losses.

The generally higher flow depths computed with the “MAX” assignment method result consequently in higher losses. Table 3 shows the computed flood losses on buildings summed up for the study area. The overall losses range from 800,000 CHF to 284 million

Table 3 Total flood losses in million Swiss Francs (CHF)

Mesh	Hazard attribution	Vulnerability function					Mean ± SD
		Totschnig et al. (2011)	Papathoma-Köhle et al. (2015)	Hydrotec (2001)	Jonkman et al. (2008)	Dutta et al. (2003)	
A	MAX	264.9	248.3	241.0	73.0	237.8	213.0 ± 78.9
	MEAN	33.2	41.9	123.5	14.0	100.1	62.5 ± 46.8
B	MAX	265.5	247.2	235.4	70.5	233.6	210.4 ± 79.3
	MEAN	21.9	28.6	103.5	10.6	81.5	49.2 ± 40.8
C	MAX	284.0	263.8	243.9	76.8	243.7	222.4 ± 83.1
	MEAN	2.9	5.0	60.5	4.9	42.3	23.1 ± 26.6
D	MAX	248.0	238.0	236.5	80.3	228.1	206.2 ± 70.7
	MEAN	0.8	1.6	38.5	2.9	26.9	14.2 ± 17.4

CHF. This is a remarkable uncertainty range and thus it underlines the importance of this sensitivity analysis. The flood loss computation is markedly sensitive to both the vulnerability function and the flow depth attribution method. While the first observation is in line with other studies (Apel et al. 2008, 2009; de Moel and Aerts 2011), the second observation adds new insights in the discussion of uncertainties in flood loss modelling. Depending on the flow depth attribution method, the total loss differs by two orders of magnitude. This can be explained by the differences in the flow depths at the single buildings. Especially, the consideration of mesh nodes within building footprint has to be avoided in averaging flow depths if these mesh nodes do not represent the z -coordinates of the ground floor but those of the roof top.

However, if only one vulnerability function and one flow depth attribution method is considered distinctly, but the mesh set-up is varied, the losses result as relatively robust. While mesh A is the most conservative in terms of number of exposed buildings and residents, it is not the most conservative in total losses. Mesh C with the “MAX” attribution method results in the highest losses.

From the viewpoint of the vulnerability functions, the one described by Jonkman et al. (2008) results in the lowest losses. This function was elaborated on data in the Netherlands. Still, the presented case study in an Alpine environment might differ markedly from a lowland situation in terms of process characteristics. The functions of Totschnig et al. (2011) and Paphoma-Köhle et al. (2015) consider torrential processes and sediment transport and might be more adequate for this case study. Nevertheless, as Cammerer et al. (2013) and Amadio et al. (2016) discussed, the transferability of vulnerability functions may be questioned in any case. However, the choice of the vulnerability function and a validation was out of scope of this study and the focus was laid on the comparison of different uncertainty sources.

From the view point of the real-world applicability, the four building representation methods applied in this work have distinct advantages and disadvantages, and the choice of method will depend on the available data and the particular application. All four methods result in computationally demanding simulations, given the grid size required to capture the complex flow between buildings. For applications that require multiple simulations or fast results, the development of computationally more efficient surrogates of these models might become necessary (Bermúdez et al. 2018). Model set-up complexity does vary significantly between the methods and is thus likely to be a more relevant criterion for choosing an approach. If a suitable DSM is available, the approach corresponding to mesh D (i.e. the BB method without building geometry data) is the easiest to implement, given that building footprints are not used to constrain the mesh. However, in order to capture precisely the contours of the buildings, a very fine grid is needed. On the other hand, methods which make use of building footprints to produce sharp elevation changes at building interfaces (meshes A and C in this work) are more demanding from a pre-processing perspective. However, they could potentially allow for a certain mesh size optimization, up to the critical grid sizes defined by building dimensions and separation distances, as noted by Fewtrell et al. (2008). This aspect is beyond the scope of this work, and no coarsening was applied in this study to ensure consistency between the four mesh configurations. The number of mesh elements can be further reduced if the buildings are represented as holes in the mesh (as in mesh A). However, this may be a disadvantage for certain applications, such as the computation of rainfall–runoff transformation from direct precipitation over the model domain. If the mesh excludes the areas covered by the buildings, the rainfall fields need to be modified to account for the artificial loss of area.

4 Conclusions

The presented model experiment allowed to assess and compare two uncertainty sources in flood loss modelling at the micro-scale. We analysed the sensitivity of a typical flood loss modelling set-up to the method for representing the buildings in the computational mesh of 2D flood models and to the method for assigning flow depths from the simulation outcomes to the single buildings.

The model experiment leads to the following main conclusions.

1. At the micro-scale, the topology between a building footprint and the computational mesh in a high spatial resolution is characterized by a high number of mesh nodes per building. Thus, the flow depths of the mesh nodes have to be interpolated in some way to assign the flow depth to the building since this parameter is needed for computing the degree of loss and consequently the loss at single building scale. As the flow depth attribution method can significantly influence the outcomes of flood loss analyses, we recommend that the chosen method is explicitly described in future studies.
2. The attribution of the maximum flow depth of all nodes within the building footprint and a specified buffer distance to the building is robust. With this attribution method, the mesh set-up (i.e. the method of representing the buildings in the computational mesh) does not significantly influence the loss estimation. In contrast, it becomes relevant when the flow depths are averaged over all nodes within the building. Herein, the nodes within the building footprint but representing the heights of the roof tops rather than the ground floor level result in flow depths of 0 m. Hence, these nodes should not be considered in averaging the flow depths. The mesh set-up should thus be designed so that it fits with the flow depth attribution method.
3. The exposure assessment is not highly sensitive to the building representation method. From this perspective, the benefits of using the more complex building representation methods in the flood inundation model are not clear. Results, however, showed that this low sensitivity to the mesh set-up is valid for the maximum flow depth attribution method only. Hence, in low-density peri-urban environments, the way how to consider the buildings in the mesh is dependent on the flow depth attribution method and thus it plays a role for exposure and flood loss estimations. Hence, further analyses should be aimed at finding a threshold for building density that acts as a proxy for areas in which the building representation method is relevant or not.

Software availability A free version of the model Iber is available for download at www.iberaula.es. The flood loss model and the procedure for processing the Iber simulation outcomes are incorporated in a Python script. The code with the functions used in this study is available at GitHub <https://github.com/zischg/IBERfloodlossmodel>. The functions follow mainly the procedure described in the method section.

Acknowledgements The authors thank the Swiss Federal Office for Statistics for providing the residential register, the Swiss Federal Office for Topography for providing the building dataset and the Canton of Bern, Switzerland for providing the Lidar terrain model. María Bermúdez gratefully acknowledges financial support from the Spanish Regional Government of Galicia (postdoctoral Grant reference ED481B 2014/156-0). Andreas Paul Zischg gratefully acknowledges financial support from the Swiss National Foundation (Grant No. IZK0Z2_170478/1).

Compliance with ethical standards

Conflict of interest The authors declare that they have no conflict of interest.

References

- Abdullah AF, Vojinovic Z, Price RK, Aziz NAA (2012) Improved methodology for processing raw LiDAR data to support urban flood modelling—accounting for elevated roads and bridges. *J Hydroinform* 14:253–269. <https://doi.org/10.2166/hydro.2011.009>
- Abily M, Bertrand N, Delestre O et al (2016) Spatial global sensitivity analysis of high resolution classified topographic data use in 2D urban flood modelling. *Environ Model Softw* 77:183–195. <https://doi.org/10.1016/j.envsoft.2015.12.002>
- Álvarez M, Puertas J, Peña E, Bermúdez M (2017) Two-dimensional dam-break flood analysis in data-scarce regions: the case study of Chipembe Dam, Mozambique. *Water* 9:432. <https://doi.org/10.3390/w9060432>
- Amadio M, Mysiak J, Carrera L, Koks E (2016) Improving flood damage assessment models in Italy. *Nat Hazards* 82:2075–2088. <https://doi.org/10.1007/s11069-016-2286-0>
- Apel H, Thielen AH, Merz B, Blöschl G (2006) A probabilistic modelling system for assessing flood risks. *Nat Hazards* 38:79–100. <https://doi.org/10.1007/s11069-005-8603-7>
- Apel H, Merz B, Thielen AH (2008) Quantification of uncertainties in flood risk assessments. *Int J River Basin Manag* 6:149–162. <https://doi.org/10.1080/15715124.2008.9635344>
- Apel H, Aronica GT, Kreibich H, Thielen AH (2009) Flood risk analyses—how detailed do we need to be? *Nat Hazards* 49:79–98. <https://doi.org/10.1007/s11069-008-9277-8>
- Arrighi C, Brugini M, Castelli F et al (2013) Urban micro-scale flood risk estimation with parsimonious hydraulic modelling and census data. *Nat Hazards Earth Syst Sci* 13:1375–1391. <https://doi.org/10.5194/nhess-13-1375-2013>
- Bellos V, Tsakiris G (2015) Comparing various methods of building representation for 2D flood modelling in built-up areas. *Water Resour Manag* 29:379–397. <https://doi.org/10.1007/s11269-014-0702-3>
- Bermúdez M, Neal JC, Bates PD et al (2017) Quantifying local rainfall dynamics and uncertain boundary conditions into a nested regional-local flood modeling system. *Water Resour Res* 53:2770–2785. <https://doi.org/10.1002/2016WR019903>
- Bermúdez M, Ntegeka V, Wolfs V, Willems P (2018) Development and comparison of two fast surrogate models for urban pluvial flood simulations. *Water Resour Manag*. <https://doi.org/10.1007/s11269-018-1959-8>
- Bladé E, Cea L, Corestein G et al (2014) Iber: herramienta de simulación numérica del flujo en ríos. *Rev Int Métodos Numéricos para Cálculo y Diseño en Ing* 30:1–10. <https://doi.org/10.1016/j.rimmi.2012.07.004>
- Bodoque JM, Amérgo M, Díez-Herrero A et al (2016) Improvement of resilience of urban areas by integrating social perception in flash-flood risk management. *J Hydrol* 541:665–676. <https://doi.org/10.1016/j.jhydrol.2016.02.005>
- Bonasia R, Areu-Rangel OS, Tolentino D et al (2017) Flooding hazard assessment at Tulancingo (Hidalgo, Mexico). *J Flood Risk Manag*. <https://doi.org/10.1111/jfr3.12312>
- Cammerer H, Thielen AH, Lammel J (2013) Adaptability and transferability of flood loss functions in residential areas. *Nat Hazards Earth Syst Sci* 13:3063–3081. <https://doi.org/10.5194/nhess-13-3063-2013>
- Cea L, Vázquez-Cendón ME (2009) Unstructured finite volume discretization of two-dimensional depth-averaged shallow water equations with porosity. *Int J Numer Methods Fluids*. <https://doi.org/10.1002/flid.2107>
- Cea L, Bermúdez M, Puertas J et al (2016) IberWQ: new simulation tool for 2D water quality modelling in rivers and shallow estuaries. *J Hydroinform* 18:816–830. <https://doi.org/10.2166/hydro.2016.235>
- Chen AS, Evans B, Djordjević S et al (2012a) A coarse-grid approach to representing building blockage effects in 2D urban flood modelling. *J Hydrol*. <https://doi.org/10.1016/j.jhydrol.2012.01.007>
- Chen AS, Evans B, Djordjević S, Savić DA (2012b) Multi-layered coarse grid modelling in 2D urban flood simulations. *J Hydrol* 470:1–11. <https://doi.org/10.1016/j.jhydrol.2012.06.022>
- Davis SA, Skaggs LL (1992) Catalog of residential depth-damage functions used by the army corps of engineers in flood damage estimation. IWR report 92-R-3, Institute for Water Resources, US Army Corps of Engineers, Ft. Belvoir, VA
- de Almeida GAM, Bates P, Ozdemir H (2016) Modelling urban floods at sub-metre resolution: challenges or opportunities for flood risk management? *J Flood Risk Manag*. <https://doi.org/10.1111/jfr3.12276>

- de Moel H, Aerts CJH (2011) Effect of uncertainty in land use, damage models and inundation depth on flood damage estimates. *Nat Hazards* 58:407–425. <https://doi.org/10.1007/s11069-010-9675-6>
- Dutta D, Herath S, Musiak K (2003) A mathematical model for flood loss estimation. *J Hydrol* 277:24–49. [https://doi.org/10.1016/S0022-1694\(03\)00084-2](https://doi.org/10.1016/S0022-1694(03)00084-2)
- Environment Agency (2014) The updated flood map for surface water (uFMfSW) property points dataset. Bristol, UK. <https://data.gov.uk/dataset/risk-of-flooding-from-surface-water-suitability>
- Ernst J, Dewals BJ, Detrembleur S et al (2010) Micro-scale flood risk analysis based on detailed 2D hydraulic modelling and high resolution geographic data. *Nat Hazards* 55:181–209. <https://doi.org/10.1007/s11069-010-9520-y>
- Fewtrell TJ, Bates PD, Horritt M, Hunter NM (2008) Evaluating the effect of scale in flood inundation modelling in urban environments. *Hydrol Process* 22:5107–5118. <https://doi.org/10.1002/hyp.7148>
- Fewtrell TJ, Duncan A, Sampson CC et al (2011) Benchmarking urban flood models of varying complexity and scale using high resolution terrestrial LiDAR data. *Phys Chem Earth* 36:281–291. <https://doi.org/10.1016/j.pce.2010.12.011>
- Freni G, La Loggia G, Notaro V (2010) Uncertainty in urban flood damage assessment due to urban drainage modelling and depth–damage curve estimation. *Water Sci Technol* 61:2979–2993. <https://doi.org/10.2166/wst.2010.177>
- Fuchs S, Birkmann J, Glade T (2012) Vulnerability assessment in natural hazard and risk analysis: current approaches and future challenges. *Nat Hazards* 64:1969–1975. <https://doi.org/10.1007/s11069-012-0352-9>
- Fuchs S, Keiler M, Zischg A (2015) A spatiotemporal multi-hazard exposure assessment based on property data. *Nat Hazards Earth Syst Sci* 15:2127–2142. <https://doi.org/10.5194/nhess-15-2127-2015>
- Fuchs S, Röthlisberger V, Thaler T et al (2017) Natural hazard management from a coevolutionary perspective: exposure and policy response in the European Alps. *Ann Am Assoc Geogr* 107:382–392. <https://doi.org/10.1080/24694452.2016.1235494>
- Garrote J, Alvarenga FM, Díez-Herrero A (2016) Quantification of flash flood economic risk using ultra-detailed stage—damage functions and 2-D hydraulic models. *J Hydrol* 541:611–625. <https://doi.org/10.1016/j.jhydrol.2016.02.006>
- González-Aguirre JC, Vázquez-Cendón ME, Alavez-Ramírez J (2016) Simulación numérica de inundaciones en Villahermosa México usando el código IBER. *Ing del agua* 20:201. <https://doi.org/10.4995/ia.2016.5231>
- Green CH (2003) *The handbook of water economics: principles and practice*. Wiley, New York
- Guinot V (2012) Multiple porosity shallow water models for macroscopic modelling of urban floods. *Adv Water Resour* 37:40–72. <https://doi.org/10.1016/j.advwatres.2011.11.002>
- Horritt M, Bates PD (2002) Evaluation of 1D and 2D numerical models for predicting river flood inundation. *J Hydrol* 268:87–99. [https://doi.org/10.1016/S0022-1694\(02\)00121-X](https://doi.org/10.1016/S0022-1694(02)00121-X)
- Hydrotec (2001) Hochwasser-Aktionsplan Angerbach (Flood action plan for the river Angerbach). Teil I: Berichte und Anlagen. Studie im Auftrag des Stua Dusseldorf. Aachen, Germany
- Jonkman SN, Bočkarjova M, Kok M, Bernardini P (2008) Integrated hydrodynamic and economic modelling of flood damage in the Netherlands. *Ecol Econ* 66:77–90. <https://doi.org/10.1016/j.ecolecon.2007.12.022>
- Kreibich H, Piroth K, Seifert I et al (2009) Is flow velocity a significant parameter in flood damage modelling? *Nat Hazards Earth Syst Sci* 9:1679–1692
- Kumar M, Bhatt G, Duffy CJ (2009) An efficient domain decomposition framework for accurate representation of geodata in distributed hydrologic models. *Int J Geogr Inf Sci* 23:1569–1596. <https://doi.org/10.1080/13658810802344143>
- McGrath H, Stefanakis E, Nastev M (2015) Sensitivity analysis of flood damage estimates: a case study in Fredericton, New Brunswick. *Int J Disaster Risk Reduct* 14:379–387. <https://doi.org/10.1016/J.IJDRR.2015.09.003>
- Merz B, Thielen AH (2009) Flood risk curves and uncertainty bounds. *Nat Hazards* 51:437–458. <https://doi.org/10.1007/s11069-009-9452-6>
- Merz B, Kreibich H, Schwarze R, Thielen A (2010) Assessment of economic flood damage. *Nat Hazards Earth Syst Sci* 10:1697–1724. <https://doi.org/10.5194/nhess-10-1697-2010>
- Notaro V, De Marchis M, Fontanazza CM et al (2014) The effect of damage functions on urban flood damage appraisal. *Procedia Eng* 70:1251–1260. <https://doi.org/10.1016/J.PROENG.2014.02.138>
- Ozdemir H, Sampson CC, de Almeida GAM, Bates PD (2013) Evaluating scale and roughness effects in urban flood modelling using terrestrial LiDAR data. *Hydrol Earth Syst Sci* 17:4015–4030. <https://doi.org/10.5194/hess-17-4015-2013>

- Papathoma-Köhle M, Zischg A, Fuchs S et al (2015) Loss estimation for landslides in mountain areas—an integrated toolbox for vulnerability assessment and damage documentation. *Environ Model Softw* 63:156–169. <https://doi.org/10.1016/J.ENVSOF.2014.10.003>
- Papathoma-Köhle M, Gems B, Sturm M, Fuchs S (2017) Matrices, curves and indicators: a review of approaches to assess physical vulnerability to debris flows. *Earth Sci Rev* 171:272–288. <https://doi.org/10.1016/J.EARSCIREV.2017.06.007>
- Qi H, Altinakar MS (2011) Simulation-based decision support system for flood damage assessment under uncertainty using remote sensing and census block information. *Nat Hazards* 59:1125–1143. <https://doi.org/10.1007/s11069-011-9822-8>
- Röthlisberger V, Zischg AP, Keiler M (2017) Identifying spatial clusters of flood exposure to support decision making in risk management. *Sci Total Environ* 598:593–603. <https://doi.org/10.1016/j.scitotenv.2017.03.216>
- Sampson CC, Fewtrell TJ, Duncan A et al (2012) Use of terrestrial laser scanning data to drive decimetric resolution urban inundation models. *Adv Water Resour* 41:1–17. <https://doi.org/10.1016/j.advwatres.2012.02.010>
- Sampson CC, Fewtrell TJ, O’Loughlin F et al (2014) The impact of uncertain precipitation data on insurance loss estimates using a flood catastrophe model. *Hydrol Earth Syst Sci* 18:2305–2324. <https://doi.org/10.5194/hess-18-2305-2014>
- Schubert JE, Sanders BF (2012) Building treatments for urban flood inundation models and implications for predictive skill and modeling efficiency. *Adv Water Resour* 41:49–64. <https://doi.org/10.1016/j.advwatres.2012.02.012>
- Staffler H, Pollinger R, Zischg A, Mani P (2008) Spatial variability and potential impacts of climate change on flood and debris flow hazard zone mapping and implications for risk management. *Nat Hazards Earth Syst Sci* 8:539–558. <https://doi.org/10.5194/nhess-8-539-2008>
- Totschnig R, Sedlacek W, Fuchs S (2011) A quantitative vulnerability function for fluvial sediment transport. *Nat Hazards* 58:681–703. <https://doi.org/10.1007/s11069-010-9623-5>
- Zischg A, Schober S, Sereinig N et al (2013) Monitoring the temporal development of natural hazard risks as a basis indicator for climate change adaptation. *Nat Hazards* 67:1045–1058. <https://doi.org/10.1007/s11069-011-9927-0>
- Zischg AP, Mosimann M, Bernet DB, Röthlisberger V (2018) Validation of 2D flood models with insurance claims. *J Hydrol* 557:350–361. <https://doi.org/10.1016/J.JHYDROL.2017.12.042>